Clinical Significance of Scintillation Camera Electronics Capable of High Processing Rates

Paul Murphy, Roger Arseneau, Eric Maxon, and Wayne Thompson

Baylor College of Medicine and St. Luke's Episcopal–Texas Children's Hospitals, Houston, Texas, and Searle Radiographics, Inc., Des Plaines, Illinois

The use of larger scintillation detectors with high-efficiency converging collimators has greatly increased the photon input rate to the crystals of scintillation cameras in many clinical studies. To process these high-count-rate data accurately, modifications have been made by some manufacturers in the electronics of scintillation cameras. Cameras with new electronic design were compared with earlier models with respect to count rate processing capability and the effect of high input rate on spatial resolution, pulse-pair pileup, image size, and instability of the amplification of energy pulses. The improvements with the new electronic design result in shorter imaging times, better preservation of resolution, increased statistical reliability, and reduced distortion of dynamic tracer curves used for quantitative analysis.

Recent advances in collimator design and detector size, combined with radiopharmaceuticals having high photon yield, have resulted in diagnostic tests that may deliver photon fluxes in excess of the levels at which scintillation cameras can process the data. Moreover, these high rates of photon input may impair certain parameters of image quality (*1,2*). For certain diagnostic tests, such as cardiac flows, input rates can exceed 300,000 cps. The observed count rate is not indicative of the input rate during such clinical tests because of variable scatter fractions and nonconstant deadtimes for scintillation cameras (*3,4*). Some of the more recent models of the Anger scintillation camera use new electronic designs that allow count rate processing capabilities up to 200,000 cps (*5*), a level that approaches the needs of standard diagnostic tests in nuclear medicine. The purpose of this study was to measure the input rates observed during routine diagnostic imaging procedures and to evaluate the effect of these input rates on camera performance and image quality.

METHODS AND RESULTS

To document the input count rates observed in routine diagnostic tests, the observed count rate and the window fraction (the fraction of the detected photons that fall within the acceptance window of the pulse-height analyzer) were measured from a series of patients undergoing imaging procedures. For low activities, the observed count rate was divided by the window fraction to determine the input rate. Higher input rates were calculated as the ratio of the activities multiplied by the low-activity count rate. Window fractions were calculated from the pulse-height spectra obtained from patients using a multichannel analyzer that sampled the pulses for all photons interacting with the scintillation camera's detector. Count rate profiles were measured for dynamic studies with the aid of a small dedicated computer by sampling the observed count rate from the entire field of view of the camera at 0.5-sec intervals. Typical maximum observed count rates and window fractions obtained during diagnostic imaging procedures are shown in Table 1. Figure 1 shows count rate curves for several dynamic flow studies performed in patients. The data in Table 1 and Fig. 1 are average values obtained from a series of approximately 10 patients in each category. The counts re-

TABLE 1. COUNT RATES AND WINDOW FRACTION FOR STANDARD IMAGING PROCEDURES

Organ	View	Activity	PG/IV	LFOV	Window-fraction (LFOV)
Brain	Ant. static	15 mCi (1 hr)	1,800 cps—HRP	2,500 cps—HRC	37–43%
	Ant. flow (35%)	15 mCi	9,000 cps—HEP	20,000 cps—HEC	37–49%*
Liver	Ant.	3.5 mCi	1,700 cps—HRP	2,000 cps—HRP 3,300 cps—HRC	27–32%
Lung	Post.	3 mCi MAA	4,400 cps—LED	18,200 cps—HEP	33–43%
	Post. (35%)	6 mCi ^{133}Xe	4,000 cps—LED	15,000 cps—HEP	41–51%
Kidney	Post.	10 mCi (3 hr)	1,480 cps—HRP	2,350 cps—HRC	32–40%
	Post. flow (35%)	10 mCi	16,000 cps—HEP	35,000 cps—HEC	30–38%*
Bone	Ant. thorax	15 mCi (3 hr)	2,100 cps—APP	4,300 cps—APP	29–36%
Heart	Ant. flow (35%)	15 mCi	35,000 cps—HEP	73,000 cps—HEC	39–46%*

20% energy window, long unblank, ^{99m}Tc radiopharmaceuticals, except as noted.
* Averaged during flow.
Collimators: HRP, HEP, APP—high-resolution, high-efficiency, all-purpose parallel-hole.
HRC, HEC—high-resolution, high-efficiency converging.
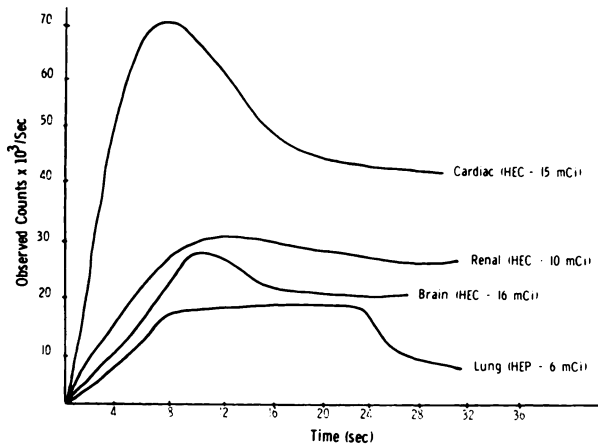LED—low-energy diverging.

FIG. 1. Observed count rate profiles for routine dynamic clinical studies with LFOV and 35% energy window. Camera operated in long-unblank mode, in which minimal separation between pulses is increased from 3.2 μsec sec (short unblank) to 12.7 μsec to permit analog-to-digital conversion for videotape data storage. Radiopharmaceuticals are labeled with ^{99m}Tc except in lung studies which use ^{133}Xe. The observed count rates for equivalent studies with small-field-of-view camera would be approximately ⅓ to ½ in magnitude. (HEC) High-energy converging; (HEP) high-efficiency parallel-hole collimator.

scintillation camera (Searle Radiographics Pho/Gamma IV) and one with the more recent electronic modifications (Searle Radiographics LFOV) were measured and are shown in Fig. 2. Note that the observed count rate maximum is considerably higher with the newer electronics.

The input rate to a scintillation camera has an appreciable effect on several parameters of image quality, for example, spatial resolution, image size, and the amount of mispositioned signals due to pulse-pair pileup. Moreover, as the count rate increases, the fraction of the full-energy peak remaining within the energy window of the pulse-height analyzer changes, thereby affecting the detection efficiency, spatial resolution, and thus the overall image quality.

To measure the change in image size with changing input rates, two ^{99m}Tc line-sources separated by

corded in these examples are those from the entire field of view of the detector. Note that in cardiac flow studies with high-efficiency converging collimation and a large-field-of-view scintillation detector, the maximum observed count rate is considerably higher than in any other tests. Typical window fractions for imaging procedures are in the range of 30–40%, indicating that on the average the camera's electronics must process three times the number of events that are eventually used to form the image.

To determine the count rate loss as a function of increasing input rate, the relationships between the observed and the true count rates of a conventional
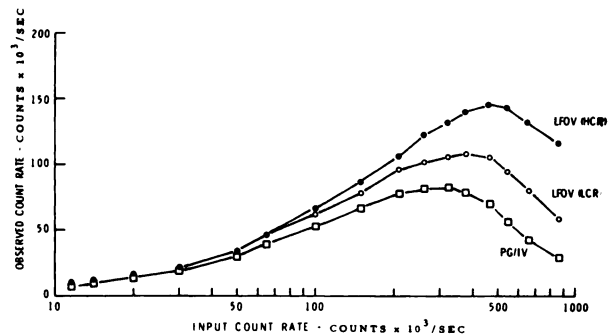

FIG. 2. Observed count rates versus input rates for two camera systems, with both systems operating in short-unblank mode and 35% energy window. With larger energy window, maximum observed count rate with LFOV is 200,000 cps. LFOV curves are shown both with high-count-rate selector switch on (HCR) and with it off (LCR). In HCR mode, integration time of positioning pulses is reduced to permit higher count rates with slight degradation of spatial resolution.

176

30 mm were imaged over the range of input rates encountered in diagnostic imaging. The distances between the peaks of the corresponding line spread functions were measured. The results for the two camera systems are shown in Fig. 3. The variation in spatial resolution with input rate was monitored by measuring the full width at half maximum of the line-source response function for ^{99m}Tc. These results are shown in Fig. 4. Note that the newer system maintains spatial resolution over a wider range of count rates while minimizing changes in image size. Changes in these two parameters are both related to baseline voltage shifts at high count rates. The data shown in Fig. 5 express the shift in the photopeak position as a function of the count rate, illustrating the substantial asymmetry in window position that can result at high count rates. This instability is due to changing gains of the photomultiplier tubes at high count rates and may prove to be one of the limiting factors in increasing the count rate capabilities of such devices. With the LFOV, an increase in photopeak pulse height at high input rates causes a larger portion of the scatter spectrum to be accepted by the pulse-height analyzer. This contributes only a small amount to the increased sensitivity of the system.

Another effect observed at high count rates is a faulty positioning of data, i.e., erroneous signals resulting from pulse-pair pileup of events that fall within the window of the pulse-height analyzer. Figure 6A illustrates this coincident effect with two point sources of radioactivity. The mispositioned signals are those between the point sources.

This positioning error occurs because the net positioning pulses are averages from the two points, weighted by the relative energies of each photon. Note that these are very obvious for the Pho/Gamma IV system but are not discernible in the LFOV. To measure the magnitude of the mispositioning effect as a function of input rate, two point-sources were separated by 15 cm at the face of the conventional detector and collimator, and the activity was increased to cover the full count rate range of the system. Point spread functions for the two point sources were stripped from the count rate profiles across the field of view of the detector to leave counts due only to coincidence events that fell within the window of the pulse-height analyzer. These events have been expressed as a fraction of the total observed counts, to yield the percent of the mispositioned events, and are shown in Fig. 6B. While this effect increases with count rate, it has little variation for different locations of the two point-sources over the face of the detector, or their separation. In comparison, the magnitude of this mispositioning artifact with the
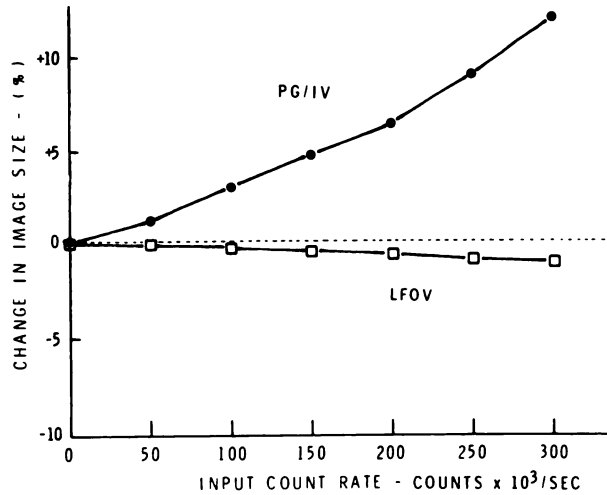

FIG. 3. Percent change in image size as function of input count rate. Size change with LFOV is much smaller in magnitude and opposite in direction to that of Pho/Gamma IV. Data obtained with 35% energy window and ^{99m}Tc.
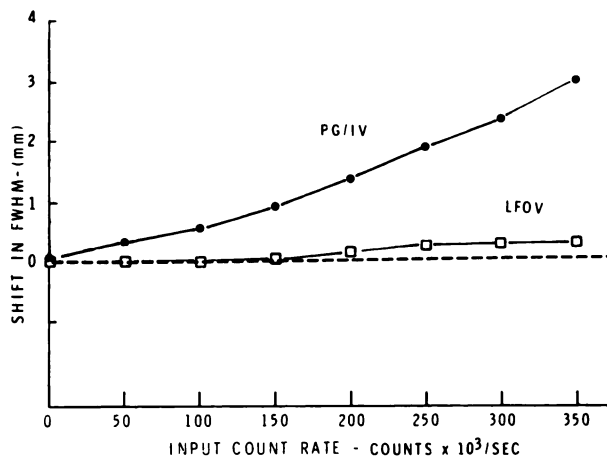

FIG. 4. Degradation in spatial resolution with increasing input rate is negligible with newer electronics (LFOV) compared to older system (P/G IV). Data obtained for 35% energy window and ^{99m}Tc.
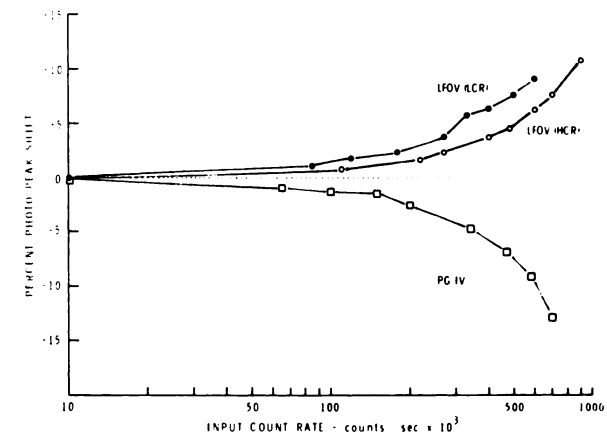

FIG. 5. Percent shift in photopeak location with respect to that at low input rates for ^{99m}Tc. LFOV results shown both with high-count-rate selector switch on (HCR) and with it off (LCR).
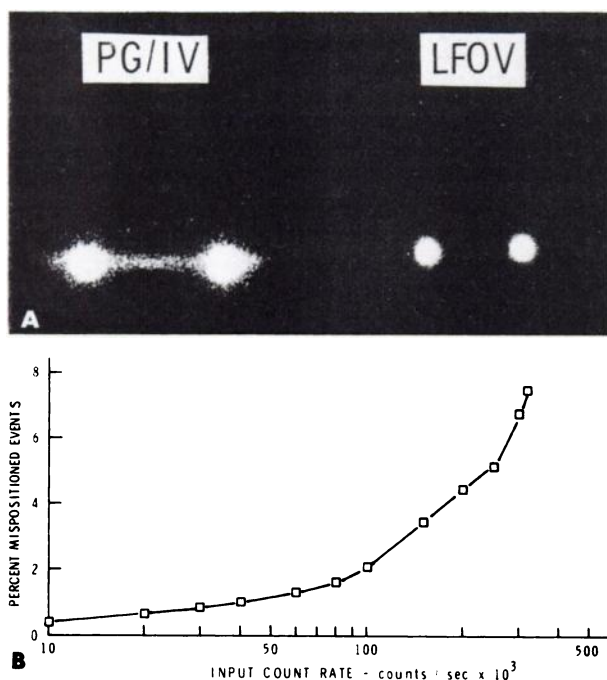
FIG. 6. (A) Mispositioned events due to coincidence detection are observed as dots between two point sources for Pho/Gamma IV, but are not discernible with the LFOV. Input count rate to both systems is approximately 200,000 cps. Data are for 20% energy window and ^{99m}Tc sources separated by 15 cm. (B) Percent of mispositioned events is shown as function of input count rate for Pho/Gamma IV. Equivalent curve for LFOV shows much less than 1% throughout all relevant input rates.

scintillation camera incorporating the more recent electronic design is much less than 1% over all observable count rates.

DISCUSSION

During most static imaging situations in clinical nuclear medicine, data collection takes place at relatively low count rates following the dilution of the administered activity in the body. In most dynamic studies only a portion of the bolus is within the field of view due to dispersion of the bolus into the various branches of the arterial circulation. In a few situations most of the radiopharmaceutical is contained within the field of view of the detector for some period of time during data collection. This occurs particularly in cardiac and pulmonary flow studies in which the injected activity has not been fractionated into vascular branches. In these circumstances the input rate to the detector may be much higher than that observed during equilibrium, with the result that the count rate acceptance capabilities of the system may be stressed. A similar situation occurs during liver and static lung imaging, although much less activity is usually administered for these tests.

With radiopharmaceuticals having high photon yield and short effective half-lives, it is not unusual

to administer 20 or more millicuries to a patient for a diagnostic test. This can result in photon fluxes in excess of the count rate capabilities of the scintillation camera when all of the activity is within the field of view. For example, approximately 650 million photons/sec are emitted from a 20-mCi ^{99m}Tc source. Approximately 325,000 photons/sec interact with the scintillation crystal, given a high-efficiency low-energy parallel-hole collimator with a detection efficiency of 5×10^{-4}. This input rate to the detector would increase with high-efficiency converging collimators (6) and would decrease with absorption of photons in overlying tissues. The net effect is to produce input rates of 300,000–400,000 cps, which demands count rate processing capabilities in this range to ensure that data are not lost.

The electronic modifications that allow these higher count rate processing capabilities include:

1. Circuitry to analyze the rise time of energy pulses, thereby permitting a priori processing for rapid rejection of very high- or very low-energy pulses that would not be accepted by the pulse-height analyzer. This reduces the deadtime for scattered events, thereby increasing count rate capabilities in the presence of scatter.

2. Buffers for temporary storage of events, placed ahead of the slower circuits. These permit acceptance of input events while slower output sections are processing prior events.

3. Circuitry for the rejection of pulse-pair pile-up to eliminate coincidence events. Piled-up events result in prolonged scintillation pulses that are rejected if they do not meet specific decay criteria.

Mispositioned pulses are noticeable in conventional cameras when there are relatively isolated areas of high activity. The phenomenon is present, however, with any distribution of radioactivity within the field of view. The problem of mispositioned data manifests itself in clinical studies as a general loss of spatial resolution. It might also be relevant in quantitative analysis, as in the calculation of cardiopulmonary parameters from the count rate curves obtained during the transit of a bolus of activity through the heart. The ability of the newer cameras to eliminate coincidence events is one of the more important contributions to improvement in image quality at high input rates.

The data in Fig. 1 demonstrate that in cardiac flow studies with high-efficiency converging collimation and a large-field-of-view scintillation detector, the maximum observed count rate is higher than in any other clinically encountered situation. The circuitry
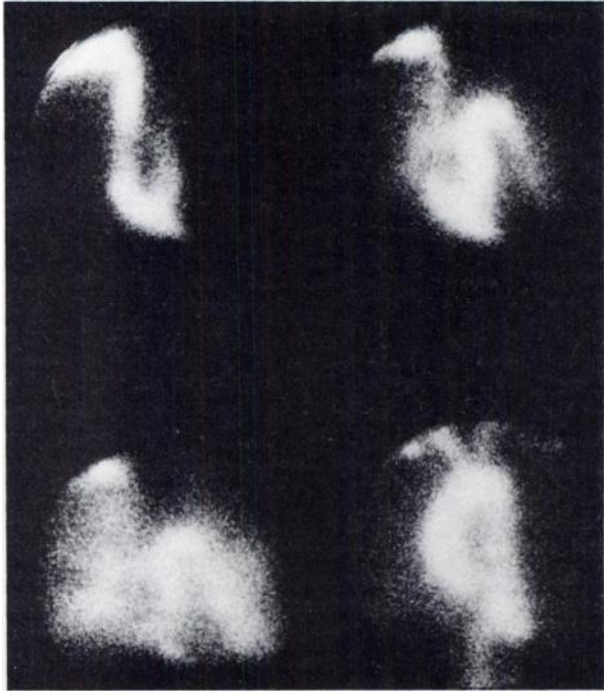
FIG. 7. Representative 1-sec frames from cardiac flow study with LFOV in short-unblank mode and with high-efficiency converging collimator. Energy window of 75% and 15 mCi of ^{99m}Tc were employed. Maximum observed count rate during this study was 154,000 cps.

in the most recent camera models includes ratio circuits with greater linearity, which, together with the coincidence-rejection feature, allow imaging with wide-energy windows, thereby permitting high-count-rate imaging with preservation of spatial resolution. The patient example in Fig. 7 illustrates this phenomenon. Cardiac flow was studied with a 75% energy window following the injection of 15 mCi of ^{99m}Tc. The maximum observed count rate during the procedure was 154,000 cps. Count rate curves from such data are 2–4 times higher than those encountered with previous camera models and are representative of curves that are being used in some institutions for the determination of parameters of cardiac function, such as ejection fraction, stroke

volume, pulmonary transit time, cardiac output, shunt detection and quantitation, and pulmonary blood and plasma volumes. Any data lost during these collection intervals could adversely affect the accuracy of such calculations due to distortion of the transit curve or due to less-than-optimal statistical accuracy for the data, particularly when small regions of interest are used.

CONCLUSIONS

The most recent vintage of Anger scintillation cameras has made available better electronic circuitry, which allows higher count rate processing capabilities, improvement in spatial resolution, elimination of pulse-pair pileup, and stability of image size at these high count rates. These advantages have significance in not only reducing total imaging time for data collection, but also in improvement of image quality and statistical reliability of quantitative analysis of dynamic flow studies.

REFERENCES

1. BUDINGER TF: High counting-rate performance of the Anger scintillation camera. *J Nucl Med* 14: 383–384, 1973
2. MORETTI JL, MENSCH B, GUEY A, et al.: Comparative assessment of scintillation camera performance. *Radiology* 119: 157–165, 1976
3. ARNOLD JE, JOHNSTON AS, PINSKY SM: The influence of true counting rate and the photopeak fraction of detected events on Anger camera deadtime. *J Nucl Med* 15: 412–416, 1974
4. SORENSON JA: Methods of correcting Anger camera deadtime losses. *J Nucl Med* 17: 137–141, 1976
5. BURDINE JA, MURPHY PH: Clinical efficacy of a large-field-of-view scintillation camera. *J Nucl Med* 16: 1158–1165, 1975
6. MURPHY PH, BURDINE JA, MOYER RA: Converging collimation and a large-field-of-view scintillation camera. *J Nucl Med* 16: 1152–1157, 1975